

# INNOVATIVE NUMERICAL PETROLOGICAL METHODS FOR DEFINITION OF METAMORPHIC TIMESCALE EVENTS OF SOUTHERN EUROPEAN VARISCAN RELICTS VIA THERMODYNAMIC AND DIFFUSION MODELLING OF ZONED GARNETS

ROBERTO VISALLI

Dipartimento di Scienze Biologiche, Geologiche e Ambientali, Università di Catania, Corso Italia, 98125 Catania

## INTRODUCTION

Innovative numerical petrology methods were developed using several computer programming languages, to investigate chemical-physical properties of metamorphic rocks at the microscale. These methods can help users to analyse the final aspect of the metamorphic rocks, which derives from the counterbalancing factors controlled by deformation *vs.* recovery processes, through a better quantification of the rock fabric parameters (*e.g.*, grain and mineral size distribution) as well as of the rock volumes and the specific compositions that take part in the reactions during each metamorphic evolutionary stage.

In this perspective, a grain boundary detection tool (*i.e.*, Grain Size Detection - GSD) was created to draw grain boundary and create polygon features in a Geographic Information System (GIS) platform using thin section optical scans as input images. Such a tool allows users to obtain several pieces of information from the investigated samples such as grain surfaces and sizes displayed as derivative maps. These maps were then integrated with the mineralogical distribution map of the entire thin section classified from the micro X-ray maps. This step was made to enhance the grain size distribution analysis by associating a mineral label to each polygon feature, by developing a further tool called Min-GSD (*i.e.*, Mineral-Grain Size Distribution).

The image analysis of rocks at the microscale was further improved by introducing a new multilinear regression technique within a previous image analysis software (*i.e.*, X-ray Map Analyser - XRMA; Ortolano *et al.*, 2014a), with the aim to calibrate X-ray maps for every classified mineral of the selected thin section microdomain. This enhancement (called Quantitative X-ray Map Analyser - Q-XRMA, Ortolano *et al.*, 2018) allowed to compute: *i*) the elemental concentration within a single phase expressed as a.p.f.u; *ii*) the maps of the end member fractions defining the potential zoning patterns of solid solution mineral phases.

Moreover, the classification through this new method of one or several microdomains *per* thin section, was able to describe the potential sequence of recognized metamorphic equilibria and was here used to a better definition of the effective bulk rock chemistries on the basis of a more robust thermodynamic modelling, providing more reliable thermobaric constraints.

These thermobaric constraints were here converted for the first time into Pressure-Temperature (*PT*) maps by the development of an add-on (*i.e.*, Diffusion Coefficient Map Creator - DCMC) of the previous tool (Q-XRMA), for creating maps of compositionally-dependent diffusion coefficients, by integrating diffusion data from the literature. As a result, an articulated Local Information System (LIS) for the investigated mineral, involving data on composition, grain size, modal amounts and kinetic rates, was created and resulted potentially useful for detailed investigations as, for instance, the determination of the timescales of metamorphic events.

All of these methods mentioned above can be considered part of “*the Petromatics*” discipline, here for the first time defined as “*the science which promotes an integrated multidisciplinary systematic approach to develop tools and techniques for detecting, handling, integrating, processing, analyzing, archiving and distributing textural-related spatial minerochemical data characterising rocks at the micro scale with continuity and in a digital format*”.

As an application, two case studies were selected for testing the methodologies described above, with the aim to derive the timescales of specific metamorphic events. In particular, paragneisses from the Serre and Sila Massifs (Calabria, Italy) were investigated applying models of compositional changes due to diffusion which are

preserved in the mineral chemical profiles, by creating LISs for millimetre almandine-rich garnets. The diffusion equation solvers were developed by coding scripts in MATLAB languages using the forward finite-difference method.

#### “PETROMATICS” AND NUMERICAL PETROLOGY SUPPORTED BY IMAGE ANALYSIS

With the advent of the digital era and increasingly performing computers, the ability to quickly obtain and quantify microstructural and minerochemical features at the microscale, through the iterative execution of numerous and complex calculations, has become increasingly larger. In particular, in recent years, the use of image processing techniques for studying rocks, has played a key role in the field of metamorphic petrology and all of the disciplines of geosciences in the broadest sense (*e.g.*, Coutelas *et al.*, 2004; Tinkham & Ghent, 2005; Friel & Lyman, 2006; Ortolano *et al.*, 2014b; Belfiore *et al.*, 2016).

In this view, several image processing tools were here developed via different programming languages, to allow quantitative extraction of various parameters characterizing rocks at the microscale, such as mineral grain size distribution, mineral modal abundances, potential mineral sub-phases occurrences, chemical concentrations and element kinetic data.

##### *Grain Size Detection (GSD): a new ArcGIS® toolbox to construct grain size distribution by drawing mineral grain boundaries on thin section scans*

The construction of the grain boundary maps is based on the acquisition of high-resolution thin section optical scans. The choice of the scan resolution was made taking into account the image quality and the related processing time. Indeed, high-resolution scans (*e.g.*, 9600 dpi) highlights straight grain boundaries better than lower ones but requires big hard drive space on a computer and more elaboration time as the pixel matrix could be huge (*e.g.*, 15000 x 9300 pixels). Conversely, low-resolution images (*e.g.*, 300 dpi) could homogenize small neighbouring grains in a unique one-saving image processing time as the smaller pixel matrix (*e.g.*, 680 x 375). Keep in mind all of these reasons, the input images (usually 38.4 x 20.6 mm in size) used to construct mineral grain size maps were acquired with a resolution of 4200 dpi, because it was considered a good compromise between image quality and hard drive space allocation on a common personal computer. Such a choice was made after several attempts at different scanner setting based on a population of more than 100 samples. Every thin section scan was successively subjected to a preliminary pre-processing phase through the Corel Graphic Suite® software, to highlight better the grain boundaries (Fig. 1a, b).

This step usually consists on brightness and contrast corrections followed by the application of the PowerTrace function of the Corel Draw® which allows reducing noise background as well.

After this step, the GSD toolbox can be launched from ArcGIS® as a new tool developed with Model Builder (*i.e.* a graphical code designer able to chart automated flow-diagram). Such a toolbox is subdivided into three different analytical routines: *i*) a pre-edge detection filter phase, able to distinguish grains from boundary lines which are identified with several colors as a consequence of an iso-cluster unsupervised classification; *ii*) an edge detection phase, able to select and refine grain boundaries; *iii*) a grain polygons creator, able to make polygons features (Fig. 1c) with specific areas and perimeters (Fig. 1d).

The developed GSD toolbox represents a valuable asset for investigating the fabric characterising deformed rocks, especially those formed by many tiny grains. Indeed, the tool permits to detect boundaries of all the grains having an area < 0.01 mm<sup>2</sup> as well. This result represents a significant improvement in the quantitative determination of the rock fabric information by the automatic digitalization of optical images.

As to the topic of diffusion, such a result is advantageous to a priori select the appropriate grains where study the elements diffusion behaviour if other conditions are satisfied (*e.g.*, if mineral can be considered cut from its centre). Indeed, according to Caddick *et al.* (2010), smaller grains change their core composition faster than the larger ones when diffusion proceeds, losing any information about the original growth chemical history. Therefore, studying the diffusive element behaviour on several grains with different grain sizes and

compositions can improve any thermobaric reconstruction as well as the timescale determination of geological events.

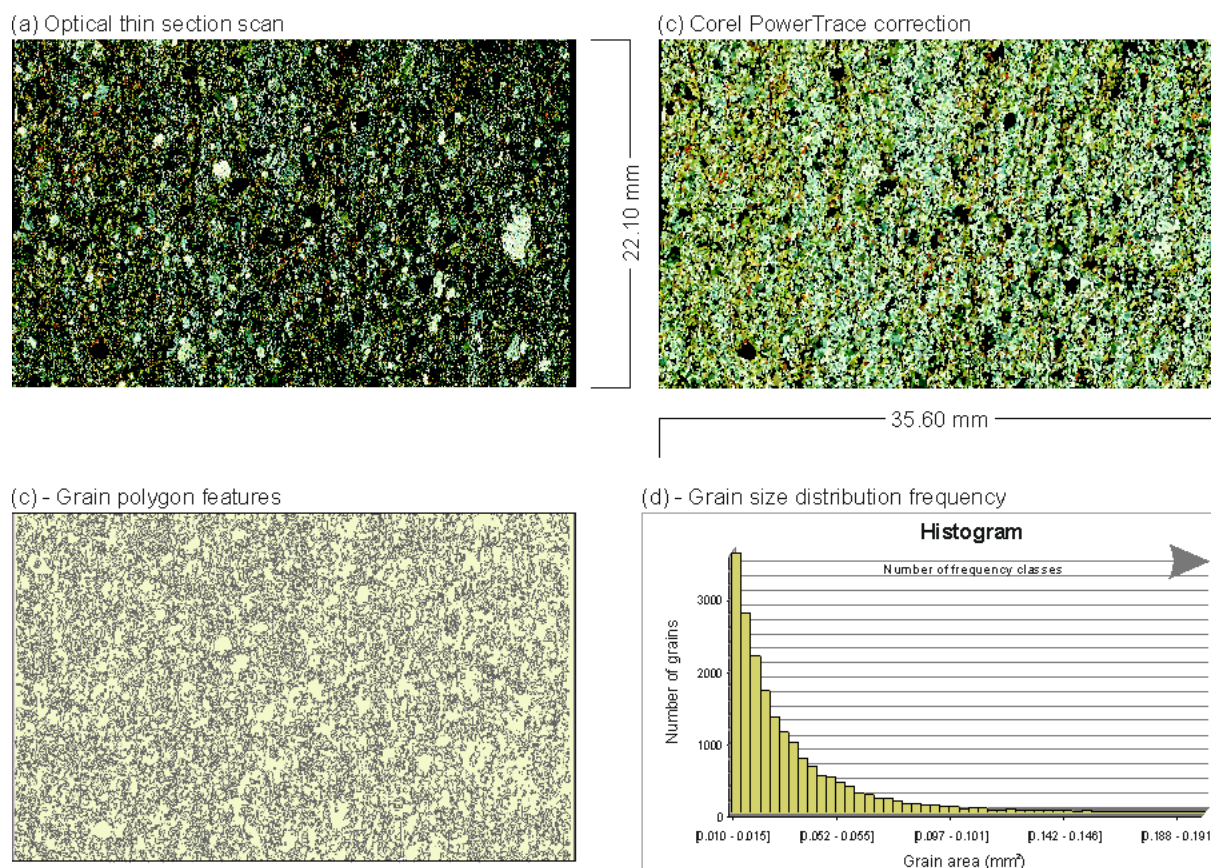


Fig. 1 - Result of the GSD ArcToolbox: a) original optical thin section; b) result of the PowerTrace Function of Corel Draw Software; c) polygon shapefile created via a feature to polygon conversion; d) histogram of the grain polygon as a function of their shape area.

#### *Quantitative X-ray Map Analyser (Q-XRMA): A new ArcGIS-based statistical approach for Mineral Image Analysis*

The second fundamental parameter that must be known to apply diffusion modelling is the chemical composition of the mineral components especially through the interface between mineral sub-phases, as well as between distinct mineral phases (*e.g.*, Garnet and Biotite), where chemical gradients could exist and therefore be modified by diffusion. On the whole, microprobe spot analyses are performed to find out these pieces of information, but recently, it is getting more use of software treating X-ray elemental maps as containers of chemical data stored as absolute values within each image-forming pixel.

In this perspective, a new ArcGIS®-based tool was developed in Python programming language with the aim of acquiring quantitative information of petrological interest using a device-independent stepwise controlled procedure, which calibrates X-ray maps *via* a regression between the element pixel intensity and the corresponding chemical concentration.

Specifically, the calibration procedure relies on a multiple linear regression technique that mirrors the interdependent element relationship constrained by the stoichiometry of the minerals. The procedure requires an appropriate number of spot analyses (*i.e.*, internal standards) providing several test indexes which allow a fast check of the calibration reliability. The native Python code (*i.e.*, X-Ray Map Analyser, Ortolano *et al.*, 2014a)

was here deeply revised and subdivided in three different cycles, now embedding: *i*) a new second analytical cycle based on a multilinear regression algorithm allowing obtaining X-ray grid images for each single recognised mineral phase; *ii*) a third analytical cycle that uses calibrated maps for the extraction of potential zoning patterns of complex solid solution mineral phases.

The multiple linear regression algorithm was here chosen because it was considered the most suitable approach to take into account the natural compositional constraints existing within each mineral due to its stoichiometry. Usually, one of the main issues in adopting a multiple linear regression approach is in finding the correct explanatory variables helping to explain the potential interdependent variation of a parameter of interest. To settle this question, the pixel intensities for major elements constituting most of the common minerals (*i.e.*, Al, Ca, Fe, K, Mg, Mn, Na, Si, Ti) were selected as explanatory variables.

The calibration procedure was based on the application of the following interdependent multiple linear regression equation:

$$[[C_i]] = \left[ (\alpha_1 [[GV_i]]_0^{255}) + (\alpha_2 [[GV_j]]_0^{255}) + (\alpha_3 [[GV_k]]_0^{255}) + \dots + (\alpha_n [[GV_n]]_0^{255}) \right] + \beta_i + \gamma_i \quad (Eq. 1)$$

Where  $[[ \ ]]$  is a discretized positive value;  $i$  represents the element of unknown concentration;  $j, k, l, \dots, n$  represent the other elements;  $[[C_i]]$  = the absolute and discretized concentrations of element  $i$  calculated for each pixel (this variable is dependent of the explanatory variables);  $\alpha_1, 2, 3, \dots, n$  = the calculated coefficients of the regression between element concentrations measured through spot analyses and the corresponding pixel intensity values of the original X-ray raster images;  $[[GV_i]]_0^{255}, [[GV_j]]_0^{255}, \dots, [[GV_n]]_0^{255}$  = the discrete pixel-intensity values of the  $i, j, k, \dots, n^{\text{th}}$ , single band elemental maps (these are independent explanatory variables);  $\beta_i$  = value of the intercept for the element  $i$ , which is the expected value of the dependent variable ( $[[C_i]]$ ) if all the independent (explanatory) variables ( $[[GV]]$ ) are zero;  $\gamma_i$  = random error for the element  $i$ , defined as the difference between measured and predicted values. The adopted calibration procedure also provides a regression report printed on the screen, filled with several statistical tests allowing to assess model performance and to evaluate the reliability of the predicted results, alerting the user with an asterisk when they give values smaller than 0.01. This warning provides the user with a fast way to check the reliability of its model.

Once the application of the calibration procedure gave satisfactory results, it permitted to extract quantitative chemical information about specific mineral phases in a few minutes and using them to derive maps of end-member fractions (Fig. 2).

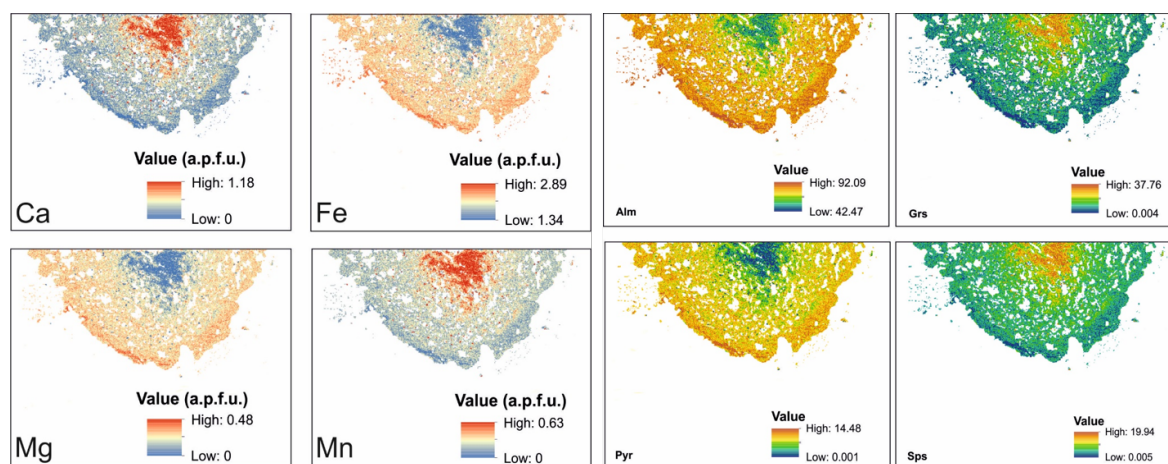


Fig. 2 - Example of Ca, Fe, Mg and Mn calibrated images and component maps derived for a garnet microdomain.

*Mineral Grain Size Distribution (Min-GSD): a useful tool to display the grain size frequency distribution of each rock-forming mineral*

Combining classification results performed in the same thin section by the Q-XRMA software on X-ray maps and the grain polygon features created by the GSD toolbox, a diagram of the grain size frequency distribution specific for the single detected mineral, can be obtained automatically. As a preliminary operation, a georeferencing of the maps under process has to be executed to ensure a perfect overlap between the two images.

After this step, the Min-GSD toolbox applies a first raster conversion of the thin section classification, obtained by the Q-XRMA, in polygon features where each polygon represents a specific mineral phase. Because of the different pixel matrix dimension of the input images and the effect linked with the georeferencing stretch, it is necessary to delimit the area enclosed within each polygon. This goal can be achieved adopting a union function which requires an initial raster to polygon conversion since the inputs required can not be a raster files. This step is followed by a minimum bounding geometry operation which allows to obtain pieces of information about the orientation of the single grains and the short and the long axis of each polygon. In such a way, a final output is obtained, where each grain polygon can be now displayed with the associated mineral name (Fig. 3a). The latter can then used to construct the diagram of the mineral grain size distribution (Fig. 3b), where the number of specific mineral grains is plotted vs. their shape areas.

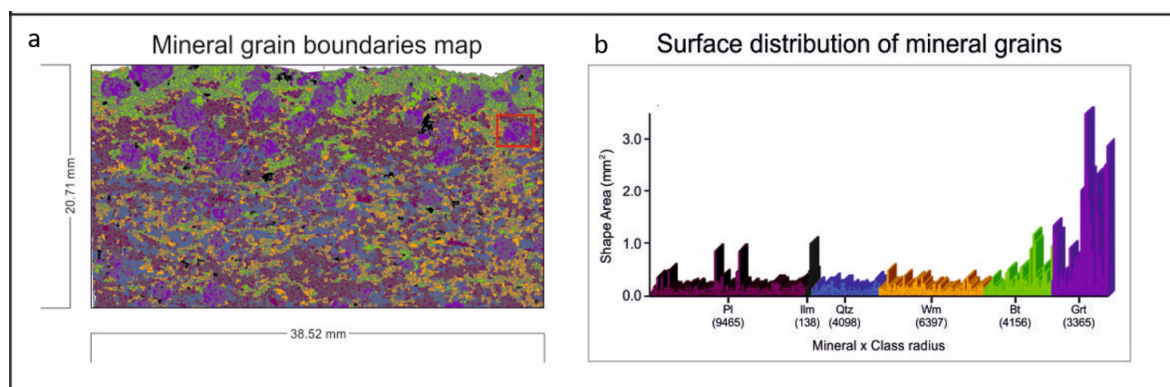


Fig. 3 - Result of the Min-GSD ArcToolbox: a) mineral grain size polygon map. All of the polygons constructed by the GSD toolbox are labelled with the appropriate mineral name classified via the Q-XRMA; b) histogram of grain size frequencies distinct for each mineral.

*Diffusion coefficient map creator (DCMC): A Q-XRMA image-processing add-on for creating map of various kinetic coefficients in a Local Information System (LIS)*

A new Python code was here implemented as an ArcGIS®-based add-on of the Q-XRMA image analysis software, with the aim to create diffusion coefficient maps (*D*-maps) of selected minerals from an investigated thin section domain. In this view, all of the three cycles of the Q-XRMA have to be executed before using the new tool. This latter allows to derive *D*-maps for garnet, but it could be extended potentially to other mineralogical phases as, for instance, olivine and plagioclase if experimental diffusion data are available. The creation of garnet *D*-maps relies on three different experimental diffusion datasets (Table 1).

The choice of these datasets comes from: *i*) the chance to investigate results carried out with old experimental data (e.g., Loomis *et al.*, 1985), by comparing them with the more recent ones (e.g., Carlson, 2006); *ii*) using the most applied data sets in literature (i.e., Carlson, 2006; Chakraborty & Ganguly, 1992); *iii*) applying diffusion data obtained by different experimental determinations.

Table 1 - Datasets of diffusion data reported in literature

Element	$D_0$ ( $m^2/s$ )	Q (kcal/mol)	$\Delta V^*$ ( $m^3/mol$ )	Activation energy (kJ/mol)	Experimental conditions	D ( $m^2/s$ ) at T = 530 °C and P = 4.2 kbar	D ( $m^2/s$ ) at T = 670 °C and P = 6.1 kbar	Study
Fe	3.10E-09	61.3		256.48 ± 35.56	T = 1300 - 1500 °C; P = 40 kbar	6.47E-25	1.94E-22	Loomis <i>et al.</i> (1985)
Mg	2.00E-09	59.9		250.62 ± 33.05		1.00E-25	2.64E-23	
Mn	2.20E-09	48.1		201.25 ± 33.05		1.79E-22	1.57E-20	
Ca	1.55E-09							
Fe	6.40E-08	65.8	5.60E-06		T = 1300 - 1480 °C; P = 14-35 kbar	5.52E-26	2.31E-23	Chakraborty & Ganguly (1992)
Mg	1.10E-07	68.0	5.30E-06			2.48E-26	1.28E-23	
Mn	5.10E-09	60.6	6.00E-06			1.15E-24	2.95E-22	
Ca	3.20E-08							
Fe	2.19E-08	63.2	1.36E-05			5.80E-26	1.7E-23	Carlson (2006)
Mg	2.17E-09	58.4	8.57E-06			1.66E-25	3.33E-23	
Mn	2.23E-08	63.2	9.63E-06			7.71E-26	2.39E-23	
Ca	1.57E-10	55.1	9.80E-06			8.58E-26	1.25E-23	

As a *a priori* condition, a domain and a mineral sub-phase classification (Fig. 4a), which can be obtained by using, respectively, the first and second cycle of the Q-XRMA, are required.

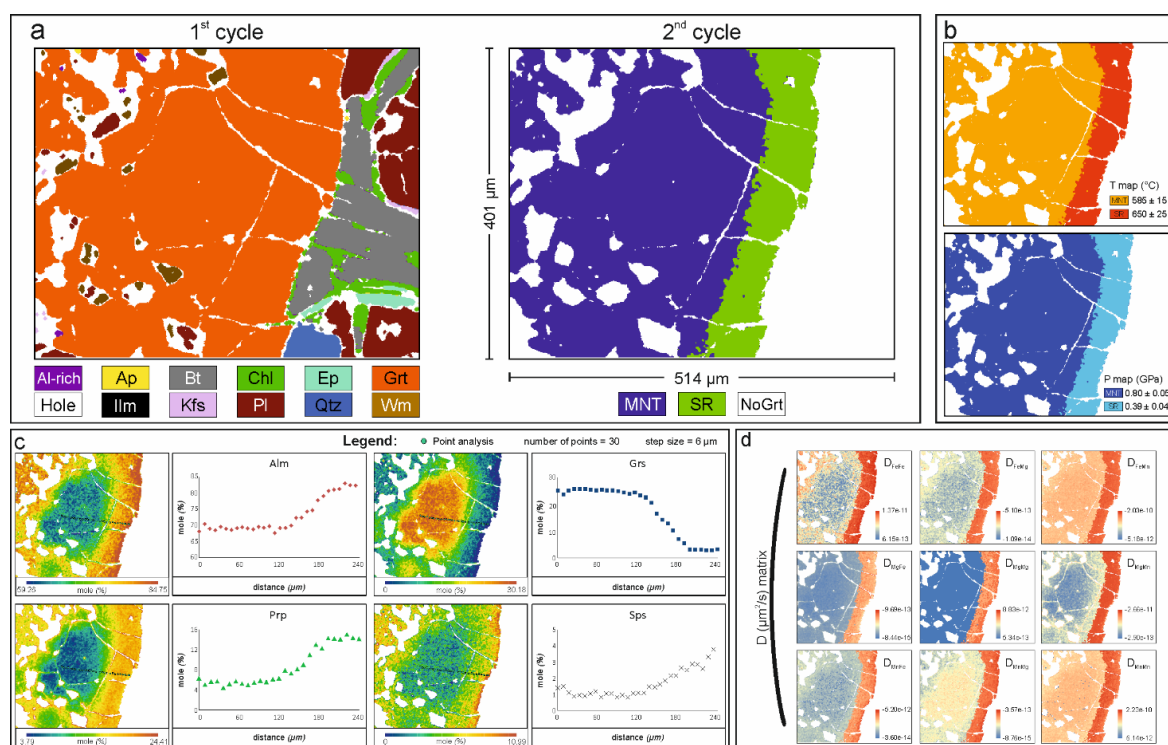


Fig. 4 - Schematic image-processing sequence to derive diffusion coefficient maps via DCMC: a) first and second cycle classification (Q-XRMA); b) temperature and pressure maps highlighting different sub-phases' values; c) third cycle quantification (Q-QRMA). A transect focussed on garnet-garnet (*i.e.*, MNT-SR) diffusion couple was derived from the maps; d) an example of a matrix of diffusion coefficients highlighting the effect of the temperature- and compositional-dependence of the kinetic coefficients.

The domain mineral classification is necessary to select a mineralogical phase to be used as a mask where execute the calculations. Moreover, the mineral sub-phases identification is used to associate, one-by-one,

temperature and pressure values linked to each sub-phase growth stage (Fig. 4b), which is required to solve Arrhenius equation in the calculation of  $D$ , expressed as follow:

$$D(P, T) = D_0 \exp((-Q - \Delta VP)/RT) \quad (Eq. 2)$$

Indeed, the add-on asks users to provide temperature and pressure information specific for every mineral sub-phase identified. As a result, maps of  $D$  expressed as a function of temperature and pressure (*i.e.*,  $D(P, T)$ -maps), are obtained. Furthermore, since the strong dependence of the element diffusivity from the mineral compositions, the add-on permits to derive maps of different chemical diffusion coefficients, such as interdiffusion coefficient, matrix of diffusion coefficients or effective binary diffusion coefficient. These outputs are obtained solving appropriate implemented diffusion coefficient equations, by using the absolute value stored in each pixel of the  $D(P, T)$  - maps and of the mineral component ones (Fig. 4c) which are derived executing the third analytical cycle of the Q-XRMA. Then, for every potential mineral investigated it is possible to obtain a database of specific  $D$ -values expressed as a function of temperature, pressure, and chemical composition, which represent the input parameters applied in diffusion modelling. The possibility to have chemical diffusion coefficient maps represents the main advantage characterising the DCMC add-on, as the compositional dependence of the kinetic coefficients requires that a new value of  $D$  should be calculated for each value of chemical concentration. Such a calculation would be an extensive time-consuming if done manually, especially in the case of a multicomponent diffusion typical of garnet, where nine coefficients must be computed at the same spot.

Figure 4d shows an example of a  $D$  -matrix constructed for a garnet at the contact between its rim (SR) and mantle (MNT) zones, highlighting as faster diffusion coefficients are localized where the garnet sub-phase grew at higher temperatures.

The DCMC tool permits, then, the user to derive a unique mineral map accompanied by an attribute table containing each information subdivided per sub-phase, such as: *i*) the atomic and component composition; *ii*) the modal abundances; *iii*) the temperature and pressure; *iv*) the element diffusion coefficient (expressed as a function of  $T$  and  $P$ ); *v*) the derived chemical diffusion coefficient. This database-format table can be considered as a part of the Local Information System (LIS) stated, in a GIS-statement similar sense, as a system designed to store, manipulate, analyze, manage, and present spatial micro petrographic data.

## CASE STUDIES

The choice of the case studies was made taking into account the possibility to investigate minerals able to keep track of their compositional changes due to diffusion, giving back reliable timescales of the different metamorphic evolutionary stages.

Following these guidelines, the case studies were selected from two different sectors (*i.e.*, Serre and Sila Massifs) of the Calabria-Peloritani Orogen (CPO). CPO is constituted by a puzzle of Variscan terranes (Cirrincione *et al.*, 2015) locally replaced by a deep-seated Alpine tectonics and finally, involved into the Alpine-Apennine thrust sheet system before the opening of the Thyrrenian basin, which controlled in turn the extensional collapse of the present-day belt.

### *First case study - Serre Massif (Southern Calabria)*

The first case study comes from the Mammola Paragneiss Complex (MPC). MPC constitutes the deeper part of the upper level of the Serre Massif, an almost continuous continental crustal section of a segment of the original southern European Variscan Belt. This is nowadays surfacing after an Alpine age tilting, which led the lowermost portion to emerge to the northern part of the Massif and the uppermost one surfacing to the south (Cirrincione *et al.*, 2015).

In this case, diffusion modelling on garnets (showing a static overgrowth rimming the relict cores formed as a consequence of a late Variscan contact metamorphism) was here applied to determine the timescale of this event. In this perspective, innovative numerical petrology methods supported by image analysis were here

applied to model the  $PT$  conditions of the static garnet overgrowth stage, by deriving quantitative maps from which extrapolate the effective bulk compositions to be used in the pseudosection construction.

A total of three pseudosections were calculated and the mineral isopleths intersections were carried out on a garnet micaschist sample.  $PT$  constraints permitted to draw a  $PT$ -path integrating and improving the previously defined one (*i.e.*, Angi *et al.*, 2010), which was affected by missing application of garnet fractionation techniques and, as a consequence, by missing of specific reliable isopleth intersections. The new  $PT$  values were, then, used in conjunction with the garnet component compositions obtained by the Q-XRMA, to acquire a suitable dataset of kinetic data to be used into the diffusion modelling. This latter was addressed via a finite-difference numerical solution as the huge number of calculations required to model very slow cationic motions characterising garnet, using minimum and maximum  $PT$  ranges derived by the thermodynamic modelling. Results of modelled profiles (Fig. 5) showed a good fit between observed and predicted concentration values defining timescales ranging from 1 to 5 Ma for the Late-Variscan contact metamorphism. Such a result testified relatively very fast heating/cooling rates (*e.g.*, averagely from 40°C/Ma to 150°C/Ma) affecting the upper crustal rocks of the Serre Massif.

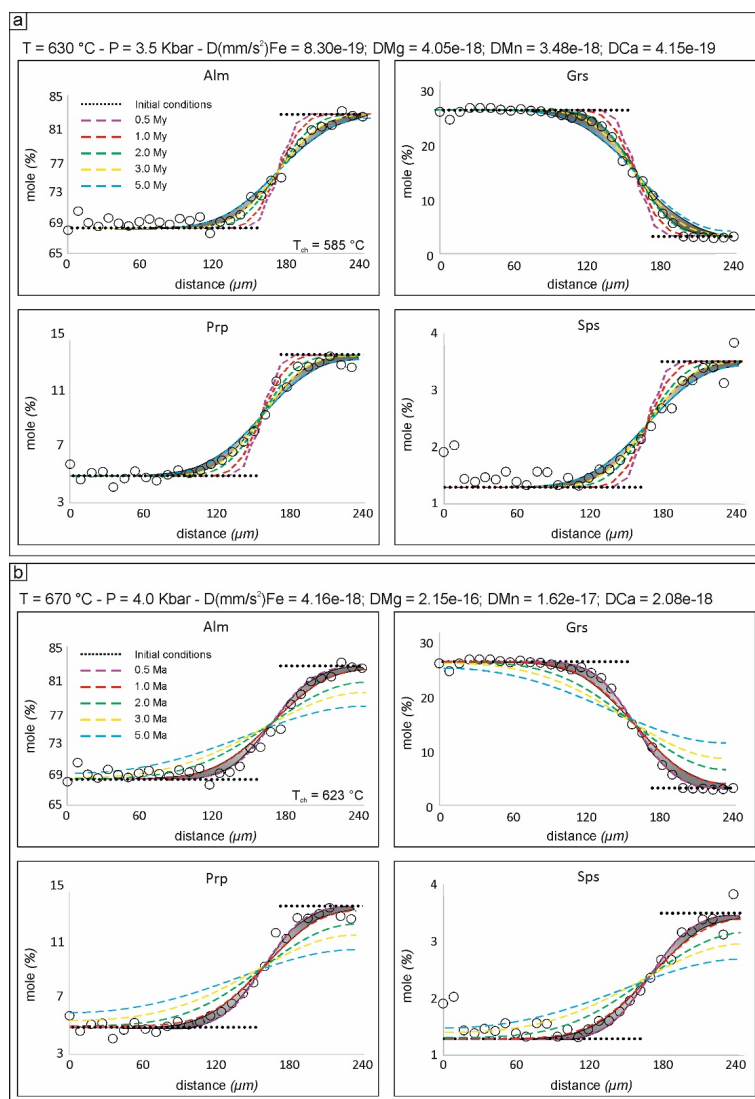


Fig. 5 - Diffusion modelling results obtained by using the minimum and maximum  $PT$  ranges derived by thermodynamic modelling. In this case, modelling garnet component provides a timescale interval of 1 to 5 Ma for the contact metamorphism. Such a range come from the strong temperature-dependence of the garnet kinetic coefficients.

### Second case study - Sila Massif (Northern Calabria)

The second case study belongs to the upper part of the deepest levels of the Sila Massif which is constituted by remnants of an almost complete crustal section of the original southern European Variscan margin. This section is currently overlapped on the Alpine oceanic derived units of the Liguride complex. Such a contact is marked, in the deepest part of the Sila crustal section, by the mylonitic horizon of the Castagna Unit. Selected samples belong to low-strain domains within these mylonites preserving memories of the original Variscan metamorphic equilibria. In this case, garnets are characterised by a flat compositional profile except for the outermost edges, where a net retrograde diffusive exchange with the surrounding matrix occurred, as highlighted by a depletion in magnesium and an iron-enrichment.

A detailed structural study combined with petrographic, thermodynamic and diffusion investigations were focused on this portion of the crystalline basement of the CPO. The *PT* pseudosections modelling performed in the low strained metapelite domains allowed reliable *PT* constraint specifically for the early retrograde stage of the metamorphic evolution. Such a result is achieved taking into account the textural equilibrium and compositional isopleth intersections among the narrow retrograde rims of the homogenized garnets and the matrix minerals such as biotite and plagioclase, considering the effect of hydration reactions as well. A reliable *PT* field (mean *P* of ~ 5.7 Kbar at *T* of ~ 630°C) was constrained by isolating the effective reactant volume *via* image analysis of the elemental X-ray maps. The diffusion model applied allowed to outline a maximum temporal estimates of about 5 Ma for the retrograde evolution, highlighting a slower exhumation with respect the shallower overlapping lithological units (Fig. 6). In this scenario, the “Castagna Unit” can be interpreted as an extensional late-to-post Hercynian shear zone, characterised by a slow cooling rate (*i.e.*, ~ 25°C/Ma) as a result of the deeper crustal position of the investigated rocks.

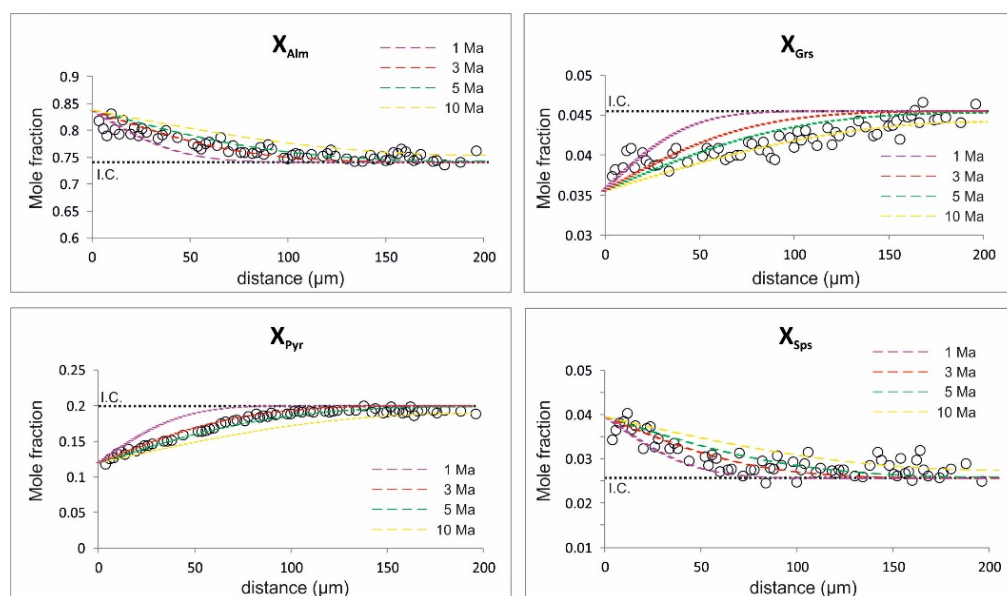


Fig. 6 - Diffusion model of the garnet retrograde zoning.  $X_{\text{Grs}}$  shows a longer timescale probable as a consequence of the slower calcium cationic movement.

## CONCLUSIONS

Innovative numerical petrology tools developed to extrapolate quantitative information about chemical-physical properties of rocks at the microscale were here combined with routinely applied thermodynamic modelling and the valuable tool of diffusion modelling, to reconstruct the pressure-temperature-time evolution

followed by the metamorphic rocks. In this context, garnet was chosen as the solid solution mineral that best records changes in *PTt* conditions, since its own common porphyroblastic fabric and slow cationic diffusion rates, making it one of the minerals most commonly used as a tracer of the *PT* trajectories of metamorphic basements (Caddick & Thompson, 2008).

The grain boundary detection toolbox (*i.e.*, GSD) allows users to draw grain polygons automatically starting from a high resolution optical thin section scan, obtaining information of grain size and areas of the investigated samples, useful to select best grain candidates for further analyses. These grain polygon maps were then integrated with the mineralogical distribution map of the entire thin section, derived from the classification of  $\mu$ -XRF elemental maps. Such a result was obtained by the development of a new toolbox (*i.e.*, Min-GSD) which enhanced the grain size distribution analysis by associating a unique mineral label to each polygon feature. This step was achieved by using a spatial join operation which put together all the attributes information stored both in the grain polygon and in the mineralogical distribution maps. As a result of this integration, a new local geodatabase (*i.e.*, a LIS) where each detected mineral grain is accompanied by geometrical and compositional data features was structured. These mineral grain size data were then integrated with those of the mineral compositions, by means of the Quantitative X-ray Map Analyser (Ortolano *et al.*, 2018). Q-XRMA permits user to extract quantitative chemical information in a few minutes without passing through additional laboratory analyses, providing, at the same time, some control indexes allowing testing the accuracy of the statistical models computed for specific elements. The classification resulting from this innovative image analysis method on one or several microdomains per thin section, could be used to a better definition of the effective bulk rock chemistries at the base of a more robust thermodynamic modelling. This definition could be achieved by the recognition of proper effective reactant volumes (*i.e.*, the real reacting volumes of each recognised metamorphic equilibria), providing, in such a way, more reliable thermobaric constraints. These thermobaric constraints were here converted into *PT* maps by the development of an add-on (*i.e.*, DCMC) of the previous tool (*i.e.*, Q-XRMA), for creating maps of compositionally-dependent diffusion coefficients, by integrating diffusion data from the literature. As a result, a complete local information system (*i.e.*, LIS) for the investigated mineral, involving data of composition, grain size, modal amounts and kinetic rates, was created and used for detailed investigation as the determination of the timescales of metamorphic events.

The application of the developed tools on two different case studies permitted to outline a timescale ranging from 1 to 5 Ma for the Late-Variscan contact metamorphism affecting the upper crustal rocks of the Serre Massif, whereas a temporal evolution of about 3-5 Ma for the retrograde evolution characterising the high-grade Castagna Unit mylonitic rocks, highlighting a slower exhumation with respect the shallower overlapping lithological units.

## REFERENCES

- Angi, G., Cirrincione, R., Fazio, E., Fiannacca, P., Ortolano, G., Pezzino, A. (2010): Metamorphic evolution of preserved Hercynian crustal section in the Serre Massif (Calabria- Peloritani Orogen, southern Italy). *Lithos*, **115**(1-4), 237-262.
- Belfiore, C.M., Fichera, G.V., Ortolano, G., Pezzino, A., Visalli, R., Zappalà, L. (2016): Image processing of the pozzolan reactions in Roman mortars via X-Ray Map Analyser. *Microchem. J.*, **125**, 242-253.
- Caddick, M.J. & Thompson, A.B. (2008): Quantifying the tectono-metamorphic evolution of pelitic rocks from a wide range of tectonic settings: Mineral compositions in equilibrium. *Contrib. Mineral. Petr.*, **156**, 177-195.
- Caddick, M.J., Konopásek, J., Thompson, A.B. (2010): Preservation of garnet growth zoning and the duration of prograde metamorphism. *J. Petrol.*, **51**, 2327-2347.
- Carlson, W.D. (2006): Rates of Fe, Mg, Mn and Ca diffusion in garnet. *Am. Mineral.*, **91**, 1-11.
- Chakraborty, S. & Ganguly, J. (1992): Cation diffusion in aluminosilicate garnets: experimental determination in spessartine-almandine diffusion couples, evaluation of effective binary diffusion coefficients, and application. *Contrib. Mineral. Petr.*, **111**, 74-86.
- Cirrincione, R., Fazio, E., Fiannacca, P., Ortolano, G., Pezzino, A., Punturo, R. (2015). The Calabria-Peloritani Orogen, a composite terrane in Central Mediterranean; its overall architecture and geodynamic significance for a pre-Alpine scenario around the Tethyan basin. *Period. Mineral.*, **84**(3B), 701-749.

- Coutelas, A., Godard, G., Blanc, P., Person, A. (2004): Les mortiers hydrauliques: synthèse bibliographique et premiers résultats sur des mortiers de Gaule romaine. *Rev. Archéom.*, **28**, 127-139.
- Friel, J.J. & Lyman, C.E. (2006): X-ray mapping in electron-beam instruments. *Microsc. Microanal.*, **12**, 2-25.
- Loomis, T.P., Ganguly, J., Elphick, S.C. (1985): Experimental determination of cation diffusivities in aluminosilicate garnets. II. Multicomponent simulation and tracer diffusion coefficients. *Contrib. Mineral. Petr.*, **90**, 45-51.
- Ortolano, G., Zappalà, L., Mazzoleni, P. (2014a): X-Ray Map Analyzer: a new ArcGIS® based tool for the quantitative statistical data handling of X-ray maps (Geo- and material-science applications). *Comput. Geosci.*, **72**, 49-64.
- Ortolano, G., Visalli, R., Cirrincione, R., Rebay, G. (2014b). PT-path reconstruction via unravelling of peculiar zoning pattern in atoll shaped garnets via image assisted analysis: an example from the Santa Lucia del Mela garnet micaschists (Northeastern Sicily-Italy). *Period. Mineral.*, **83(2)**, 257-297.
- Ortolano, G., Visalli, R., Godard, G., Cirrincione, R. (2018): Quantitative X-Ray Map Analyser (Q-XRMA): A new GIS-based statistical approach for Mineral Image Analysis. *Comput. Geosci.*, **115**, 56-65.
- Tinkham, D.K. & Ghent, E.D. (2005): XRMapAnal: a program for analysis of quantitative X-ray maps. *Am. Mineral.*, **90**, 737-744.